A REVIEW OF MULTIPLE AMPLITUDE-PHASE DIGITAL SIGNALS[1]

JOEL G. SMITH
Jet Propulsion Laboratory
California Institute of Technology
Pasadena, CA.

Summary This paper reviews the data rate, error rate, and signal-to-noise ratio relationship for various uncoded M-ary digital amplitude modulation (AM), phase modulation (PM), and combined AM-PM systems. These signal systems have the common virtue that expanding the number of possible signals to be transmitted increases the data rate but not the bandwidth. The increased data rate generally requires an increased signal-to-noise ratio to maintain constant error probability performance. Thus, these systems use power to conserve bandwidth.

A general treatment of the error rate of M-ary digital AM-PM permits development of a simple yet accurate expression which approximates the increase in average signal-to-noise ratio (over that of binary phase shift keying) required for constant error performance. This equation provides insight into why arrays differ in their signal-to-noise ratio requirements.

Introduction In any bandwidth-constrained digital communication environment, uncoded M-ary amplitude-and-phase modulation systems must be considered as a means of increasing data rate without expanding bandwidth. These may be simple M-ary amplitude shift keying [1-3] or M-ary phase shift keying (PSK) [2-7], systems with independent amplitude-and-phase shift keying [8-9], systems with two amplitude shift keyed sets in quadrature (QASK) [10], single sideband ASK [11-12], or any of a large number of combined dependent amplitude-and-phase shift keying [13-18].

An uncoded M-ary digital communication system transmits once every signaling interval T one of M possible signals corresponding to one of M information symbols (0,1,2,...,M - 1). It is assumed that successive symbols, and thus, successive signals, are independent and

[1] This paper presents the results of one phase of research carried out at the Jet Propulsion Laboratory, California Institute of Technology, under Contract No. NAS 7-100, sponsored by the National Aeronautics and Space Administration.

equally likely. An M-ary amplitude-and-phase shift-keyed (MAPSK) system transmits in each interval T signals of the form[2]

$$s_i(t) = \mathrm{Re}\left\{ s_i \sqrt{2}\, e^{j\omega_o t} \right\}, \qquad \omega_o \gg 2\pi/T \tag{1}$$

where "Re" denotes "the real part of," and phasor s_i takes on one of M complex values corresponding to the M possible symbols

$$s_i = A_i e^{j\theta_i} = X_i + jY_i \tag{2}$$

Thus the power in the signal $S_i(t)$ is

$$S_i = |s_i|^2 = A_i^2 = X_i^2 + Y_i^2 \tag{3}$$

and a signal $s_i(t)$ can be pictorially displayed as a phasor (or signal point) s_i in a two-dimensional plane, where the square of the distance from the origin to s_i is the power in $s_i(t)$. A signal set is an array of signal points

$$S \triangleq \frac{1}{M} \sum_{i=0}^{M-1} S_i \tag{4}$$

In any signaling interval T, the transmitted signal $s_i(t)$ is perturbed by a sample of a zero mean white Gaussian noise process n(t) of one-sided spectral density N_o W/Hz, and the received signal is $r(t) = s_i(t) + n(t)$. The receiver's function is to detect in each interval which one of M signals (and hence what symbol) was sent. The receiver is assumed to know the frequency ω_o and the signaling interval, as well as the a priori possible values of s_i. This assumes frequency synchronization, symbol synchronization, carrier synchronization, signal ambiguity resolution, and amplitude control. In the maximum-likelihood receiver, the received signal is correlated with two quadrature reference signals to obtain a phasor representation of the received signal and the signal selected whose phasor is closest to the received phasor in the two-dimensional signal plane. Thus, the signal space may be subdivided into exclusive and exhaustive decision regions R_i, each containing a signal point s_i. The decision region R_i is chosen such that if a noisy signal point lies in the region of s_i, the corresponding signal $s_i(t)$ was most likely sent. The decision region for each signal point is that set of all possible points closer to that signal

[2] In practice, the signals may be shaped by a time function to yield a better spectral profile than that of the rectangular pulse. The resulting signal may or may not be restricted to one signaling interval. This aspect of the signal design is ignored here by relating all performance to that of binary PSK. This approach focuses attention on the real bandwidth-conserving effects of M-ary communication, rather than on those of the various spectral shaping techniques.

point than to any other. A region R_i is determined by the intersection of semi-infinite regions R_{ij} containing s_i and bounded by the perpendicular bisector of the line connecting s_i to its neighboring points s_j ($j \neq i$, $j = 0,1,2,...,M - 1$). The correlator outputs U and V are statistically independent Gaussian random variables with means X_i and Y_i respectively and identical variance $\sigma^2 = N_o/2T$. The point (U, V) is the noisy signal point. The region R_i in which (U, V) lies contains a signal point s_i, which is the most likely to have been sent.

The first few figures show the geometric arrays of a variety of MAPSK systems.[3] Figures 1 and 2 show the simple multiple amplitude shift keyed (MASK) and multiple phase shift keyed (MPSK) systems respectively. The linear array of MASK is characterized by phasors $s_i = A_i \exp(j\theta_o)$, $i = 0,1,2,..., M - 1$, while the circular array of MPSK is characterized by phasors $s_i = A_o \exp(j\theta_i)$, $i = 0,1,2,..., M, - 1$. That is, these two systems may be categorized as type 0 systems in which only one of the two parameters (amplitude or phase) is varied.

Historically, arrays of the kind shown in Figure 3 have been labeled Type I [13]. This is a signal system with independent amplitude and phase shift keying (IAPSK). The amplitude ranges over K possible values A_k, $k = 0,1,..., K - 1$, while the phase independently ranges over L possible values so that M = KL. The independence of phase and amplitude in IAPSK systems forces the use of the same phases in each of the concentric rings. The Type II [13] signal systems of Figure 4 represent the earliest attempt to remove the restriction of the same phases for all amplitude levels. The system consists of an inner level with three phases, with each successively larger ring containing six more phases than the one prior. Quadrature amplitude shift keying (QASK), historically called Type III [10], is a signal system consisting of two quadrature ASK signals. That is, in each signaling interval two signals in quadrature are independently amplitude modulated. As shown in Figure 5, the array is one of concentric squares, at least when M is the square of an integer. For values of $M = 8,32,128,..., 2^{2n+1}$, rectangular arrays of independent quadrature signals may be used, although more complicated arrays are possible [10].

Finally, in Figures 6 through 10 are shown arrays which may be called Type IV. These are arrays in which neither phase-amplitude or quadrature component independence nor the restriction to circular patterns is retained. The arrays may include signal points at the origin, as in the arrays of concentric pentagons or hexagons of Figures 8 and 9. The arrays may be complete concentric polygonal arrays such as the diamonds of Figure 7, the pentagons of Figure 8, or the octagons of Figure 10; or incomplete (when restricted to dyadic numbers 4, 8, 16, 32, 64,...) polygonal arrays such as the concentric triangles of Figure 6 or concentric hexagons of Figure 9. Many other arrays are possible and have been considered elsewhere (see especially [15]).

[3] The points represent the actual signal points, the solid lines indicate the maximum-likelihood decision regions, and the dashed lines indicate the regularity of signal structure.

In successive sections, the performance of systems based on these various signal sets is examined in terms of the geometric patterns. The average power performance depends roughly on how well the points cluster around the origin, yet remain separated from one another. The Gilbert approximation [19] to the probability of error is linearized to provide a simple but accurate expression relating the "clustering" and "separation" characteristics to the increased average signal-to-noise ratio necessary to maintain constant error performance. The relative performance of the systems is shown by plotting the data rate achievable (relative to binary PSK) as a function of the average signal-to-noise ratio (relative to binary PSK) at constant error rate and bandwidth. Asymptotically, as the number M of signals increases, type 0 systems in which only one parameter (amplitude or phase) is modulated require a 6-dB increase in average signal-to-noise ratio to achieve a doubled data rate at constant error rate, while Types I, II, III, and IV with joint modulations of both parameters all require only a 3-dB increase.

M-ary APSK Error Rate Expressions For most signal sets of regular structure, the least of the distances from each signal point in an array to its nearest decision region boundary is a measure of how tightly the signal points are "clustered." This minimum distance, called the "Gilbert distance," is denoted here by δ. The ratio of the average signal power S of an array to the squared Gilbert distance δ^2 is called the "packing coefficient" C_p of the array and is a measure of how tightly the signals are "packed" around the origin; i.e.,

$$S = C_p \delta^2 \tag{5}$$

Since the received signal phasor U + jV is the signal point s_i plus a two-dimensional independent Gaussian noise random variable of mean zero an variance ($\sigma^2 = N_o/2T$, it is convenient to normalize the space of signal points by the scale factor $1/\sigma$. Denoting the normalized Gilbert distance by $\Delta = \delta/\sigma$, the average symbol signal-to-noise ratio $R_d \triangleq ST/N_o$ is given by

$$R_d = \frac{C_p}{2} \Delta^2 \tag{6}$$

In the normalized signal space, the signal s_i has coordinates (x_i, y_i) and maximum-likelihood decision region R_i with complement $\overline{R}_i$. If for each value of i, the signal point s_i is translated to the origin and R_i denotes the corresponding translation of the maximum-likelihood region R_i, then the conditional probability of error is

$$p(e/i) = \frac{1}{2\pi} \int_{\overline{R}_i} \exp\left[-\frac{1}{2}\left(x^2 + y^2\right)\right] dx\, dy \tag{7}$$

The average probability of symbol error p(e) can now be calculated since all the signals are equally probable by

$$p(e) = \frac{1}{M}\sum_{i=0}^{M-1} p(e/i) \tag{8}$$

The conditional probability p(e/i) may or may not be convenient to evaluate, depending on the shape of the region $\bar{R}_i$. Since R_i is the intersection of M - 1 semi-infinite planes $\bar{R}_{ij}$ $j \neq i$, then $\bar{R}_i$ is the union of the complements of these planes, $\bar{R}_{ij}$.. The "union" bound on p(e/i) is obtained by assuming that the regions $\bar{R}_{ij}$ are disjoint and that

$$p(e/i) = \sum_{j \neq i} Q(\Delta_{ij})$$

where $2\Delta_{ij}$ is the (normalized) distance between the ith and jth signal point, and $Q(\Delta_{ij})$, the probability of lying in the jth region $\bar{R}_{ij}$ when the ith signal was sent is

$$Q(\Delta_{ij}) \triangleq \frac{1}{\sqrt{2\pi}}\int_{\Delta_{ij}}^{\infty} \exp\left(-\frac{1}{2}x^2\right) dx \tag{9}$$

Thus, the probability of error p(e) can be bounded by

$$p(e) < \frac{1}{M}\sum_{i=0}^{M-1}\sum_{j \neq i} Q(\Delta_{ij}) \tag{10}$$

The "Gilbert" approximation [19] of p(e) is based on a recognition that for most signal sets $Q(\Delta_{ij})$ is negligible at high signal-to-noise ratios except for the minimum Δ_{ij}, that is, the (normalized) Gilbert distance Δ.

The Gilbert number N is defined [19] as the average number of adjacent signal pairs at the Gilbert distance Δ. The Gilbert approximation of p(e) is

$$p(e) \cong NQ(\Delta) \tag{11}$$

An even grosser but still useful bound on p(e) is the "spherical" bound, in which each decision region is replaced by a circle of radius Δ with center at the signal point. Transformation to circular coordinates and integration outside the circle of radius Δ yields the "spherical" bound on p(e):

$$p(e) < e^{-\Delta^2/2} \tag{12}$$

This bound, while crude, is illuminating! If the array of signal points is considered, each centered at a circular decision region of radius Δ, this bound on the probability of error depends only on the radius Δ, as does the average signal-to-noise ratio R_d The signal array can be viewed as a collection of spheres of radius Δ in a two-dimensional plane. Holding the spheres constant in size is equivalent to holding the probability of error constant. The spheres may be shifted around on the plane without affecting the error bound. Squeezing the spheres as tightly as possible around the origin has the effect of minimizing the average signal-to-noise ratio. If binary PSK (with unity packing coefficient) requires an average signal-to-noise ratio R_{do} to achieve a specified symbol error rate p, and an arbitrary MAPSK array with packing coefficient C_p requires R_d to achieve the same p, then using equations (6) and (12) reveals that

$$C_p = \frac{R_d}{R_{do}} \tag{13}$$

That is, **the packing coefficient is the average signal-to-noise ratio (relative to binary PSK) required to transmit M-ary information at a constanterror-rate spherical bound!**

Since the bound is meaningful only for high signal-to-noise ratios, a somewhat tighter estimate, the Gilbert approximation, can be used, but the symbol error rate must be specified. The Gilbert number for M-ary ASK is N = 2(1 - 1/M) since all but the extreme two signal points have two adjacent signal points. Binary PSK has a Gilbert number of 1 while MPSK's Gilbert number is N = 2. For Type I IAPSK (K, L) the Gilbert number is N = 2, since signal points in the innermost ring have three adjacent signal points, those in the outermost ring have only one, while those of the remaining K - 2 rings have two. For QASK (K^2) with four "corner" points, each with two nearest neighbors, $(K - 2)^2$ "interior" points each with four nearest neighbors, and 4 (K - 2) "side" points, each with three nearest neighbors, the Gilbert number N is = 4(1 - 1/K). More generally, for rectangular QASK (K, L) it is easy to show that the Gilbert number N = 4(1 - (K + L)/2KL). Setting the probability of error p constant establishes the binary PSK signal-to-noise ratio R_{do} according to the formula $p \doteq Q(\sqrt{2R_{do}})$, and the signal-to-noise ratio R_d of any signal set according to the formula $p = NQ(\sqrt{2R_d/C_p})$. Note that if the effect of the Gilbert number is neglected (N = 1), equating the two formulas yields the packing coefficient $C_p = R_d/R_{do}$ as before.

It is also possible to find the increased signal-to-noise ratio of an M-ary APSK array (relative to binary PSK) in terms of the packing coefficient and Gilbert number through use of the Gilbert estimate. Letting Δ_o denote the Gilbert distance of binary PSK that achieves Gilbert approximation to p at signal-to-noise ratio R_{do}, and Δ the Gilbert distance of the M-ary APSK array at ratio R_d and the same p, then

$$p = Q(\Delta_o) = NQ(\Delta)$$

Taking natural logarithms of both sides, assuming that log [Q(x)] is linear in x and that

$$Q(x) \simeq \exp(-x^2/2)/\sqrt{2\pi x^2},$$

yields

$$\Delta \simeq \Delta_o + \frac{\log N}{\Delta_o} \tag{14}$$

Now, using equations (6) and (14) for both arrays,

$$C_p \simeq \frac{R_d}{R_{do}}\left[1 - \frac{\log N}{R_{do}} + \frac{3 + \log N/R_{do}}{\left(1 + \frac{2}{\log N/R_{do}}\right)^2}\right] \tag{15}$$

The value of N must be less than 6, since that is the most nearest neighbors a point can have. For $p \leq 10^{-4}$, $R_{do} \geq 7$, and $\log N/R_{do} \leq 1/4$. Under these conditions the third term is negligible relative to the second and may be discarded. The assumption that $p \leq 10^{-4}$ is essential also to the assumption of linearity of log [Q(x)] and Q(x) taking on its asymptotic form. Likewise $N < 6$ makes the linear assumption more believable. Thus, the signal-to-noise of an M-ary APSK array, relative to binary PSK, can be described in terms of its packing coefficient C_p and Gilbert number N at a prescribed probability level $p = Q(\sqrt{2R_{do}})$ by use of the Gilbert approximation to achieve

$$\frac{R_d}{R_{do}} \simeq \frac{C_p}{1 - \frac{\log N}{R_{do}}} \tag{16}$$

Again, if the Gilbert number effect is neglected (N = 1), equation (16) reduces to equation (13) derived from the spherical bound. Equation (16) has been applied to several 4-bit M-ary APSK arrays (Types 0, III, and IV) which had been exactly evaluated at 10^{-5} [17] and found to be less than 0.1 dB in error in all cases.

More precise performance analysis is possible, though not necessary for purposes of comparison between Types 0, I, and III systems. The exact error performance for MASK in fact equals the Gilbert approximation. The Gilbert approximation for MPSK essentially neglects the overlapping region opposite the origin of two semi-infinite regions (see, for examples, Figures 13 and 14 of [2]). For quadriphase, this amounts to approximating $2Q(\Delta)[1 - Q(\Delta)]$ by $2Q(\Delta)$, a small error at high signal-to-noise ratio. At higher values of M, the effect will be even less. Likewise, for IAPSK (K, L), if the regions are approximated by rectangles and semi-infinite strips, the probability of error becomes

$NQ(\Delta)[1 - Q(\Delta)/K]$, which can be approximated as before by $NQ(\Delta)$. The Type III QASK (K^2) has sufficiently well-shaped maximum-likelihood decision regions to permit an analytic solution to the exact error performance. The exact probabilities of symbol error, given that "corner," "interior," and "side" points are transmitted, are $Q(\Delta)[2 - Q(\Delta)]$, $4Q(\Delta)[1 - Q(\Delta)]$. and $Q(\Delta)[3 - 2Q(\Delta)]$, respectively, and thus,

$$p(e) = 4\left(1 - \frac{1}{K}\right)Q(\Delta)\left[1 - \left(1 - \frac{1}{K}\right)Q(\Delta)\right] \tag{17}$$

where Δ is the (normalized) Gilbert distance as before. Recalling that the Gilbert number N for QASK (K^2) is $4(1 - 1/K)$, the probability of error can be written as $p(e) = NQ(\Delta)[1 - NQ(\Delta)/4]$, and the Gilbert approximation $p(e) = NQ(\Delta)$ is quite adequate at large signal-to-noise ratio. Exact expressions for MPSK are available in the literature [7].

M-ary APSK Error Rate Performance In an MASK system with M signals uniformly spaced on interval (-A, A), the separation between all adjacent points is the same, the Gilbert distance $\delta = A/(M - 1)$, the M amplitudes $A_i = (M - 1 - 2i)\delta$, i = 0,1,2,..., M 1, and thus, using equations (3) (4) and (5) the packin coefficient is

$$C_p(M) = (M^2 - 1)/3$$

In an MPSK system with M signals uniformly spaced around a circle of radius $A_o = \sqrt{s}$, the separation between all adjacent points is the same $2A_o \sin \pi/M$, the Gilbert distance $\delta = A_o \sin \pi/M$, and thus

$$C_p(M) = \csc^2 \pi/M$$

In a Type I (IAPSK) system with M signals arrayed with L uniformly spaced phases at K amplitudes A_i, i = 0,2,..., K - 1, the distance between adjacent signals in the inner circle is $2\, A_o \sin \pi/L$. If this is set as the minimum signal separation, the Gilbert distance δ is $A_o \sin \pi/L$, and placing the outer circle s at $A_i = A_o + 2i\delta$, i = 1,2,..., K - 1, minimizes the packing coefficient without reducing the Gilbert distance. Thus, the K levels are $A_i = (\csc \pi/L + 2i)\delta$, i = 0,1,2,..., K - 1, and the packing coefficient is

$$C_p(K, L) = \csc^2 \pi/L + 2(K - 1) \csc \pi/L + 2(K - 1)(2K - 1)/3$$

when M is a perfect dyadic square, the best number of phases is four times the number of power levels, and

$$C_p(M) \simeq 4M/3 - 2.275 \sqrt{M}$$

In the Type II system, the K amplitude levels are $A_k = 2(1/\sqrt{3} + k)$, k = 0,1,2,..., K - 1, while the number of phases $n_k = 3(1 + 2k)$, k = 0,1,2,..., K - 2. The outer ring will generally not be completely filled since the total number of signal points is usually a dyadic integer (2,4, 8,16,32,...) and no ring is completely filled by any of these numbers (L rings contain $3L^2$ points). This incomplete outer ring makes it difficult to characterize the packing coefficient analytically. However, asymptotically the packing coefficient is

$$C_p(M) \simeq 2M/3 - 1.8\sqrt{M}$$

which is approximately an asymptotic 3-dB improvement over that of the Type I system.

In a QASK system with M signals arrayed as K and L uniform amplitudes in quadrature each level se arated by 2δ, the packing coefficient is

$$C_p(K,L) = (K^2 - 1)/3 + (L^2 - 1)/3$$

For a fixed value of M, the minimum C_p occurs for $K^2 = M$. Thus, when M is a perfect square,

$$C_p(M) = 2(M - 1)/3$$

Once it is recognized that efficient use of average signal-to-noise ratio is achieved by minimizing the packing coefficient for a fixed number of points, then a large variety of sphere-packing arrangements is possible. The Type II system of Lucky and Hancock has little more than historical significance, since it does not perform as well as the Type III QASK yet is much more difficult to implement. The pentagonal array (Figure 8) was apparently considered independently by three different researchers as a “natural” collection of 16 points. That is, initial searches for good arrays tend to look for “complete” circular patterns, although in fact the completeness has no relevance at all. The octagonal array (Figure 10) is achieved by rotating the outer ring of a Type I system and nesting it as close as possible to the inner ring without reducing the Gilbert distance. The various triangular, diamond-shaped, and hexagonal arrays (Figures 6, 7, and 9) are based on a recognition that the tightest possible sphere packing uses equilateral triangular structures to characterize signal point geometry. All three systems have hexagonal decision regions. The primary difference between the three sets is simply placement of the various arrays relative to the origin -- or, in any large isometric array of hexagonal regions, where the origin is placed. For concentric hexagons, there is one signal at the origin, while for concentric triangles, there are three signals around the origin, and for concentric diamonds, there are four signals (in a complete diamond) around the origin.

The packing coefficient for complete concentric triangles and diamonds is $C_p(M) = 2(M - 1)/3$ and slightly less for concentric hexagons [17]. Note that this is the same packing coefficient as for QASK for the same number of signal points, and that the diamonds are simply “squished” squares. In fact, it can be shown that any array of concentric rhombuses has the same power independent of the angles, and that for any angle between the right angles of QASK and the angles of the diamonds, the packing coefficient is unchanged, although not the Gilbert number N.

Figures 11, 12, and 13 show the relative performance of the several arrays discussed. Figure 11 plots the data rate (relative to binary PSK)[1] versus the average symbol signal-to-noise ratio (relative to binary PSK) at constant spherical error bound. In Figure 12 the plot is made with the Gilbert approximation at 10^{-5}. In Figure 13, the abscissa is divided by M to show the average bit signal-to-noise ratio (relative to binary PSK), at constant bit error. The bit error is taken as the symbol error divided by $\log_2 M$, which assumes perfect two-dimensional Gray coding and negligible Gray code penalty [17]. The performance curves of the various Type IV systems are indicated by the shaded region around QASK.

The asymptotic performance of the Type 0 MASK and MPSK signal sets shows a four-fold increase in signal-to-noise ratio required to double the data rate at constant error performance. This follows from the asymptotic M^2 form of the packing coefficient. The Types I through IV, on the other hand, have packing coefficients which are asymptotically linear in M and thus require only a doubled signal-to-noise ratio.

Conclusions M-ary amplitude-phase shift keyed (MAPSK) signal sets are appropriate in an average-power-and-bandwidth-constrained communication environment. The historical development of the various types of signal sets has been traced from the simple Type 0 systems to the fairly complex Type IV. The concepts of the Gilbert distance and packing coefficient have been introduced to permit insight into the relative performances of the various signal systems under an average signal-to-noise ratio constraint. Bounds on error rates have been examined to relate the effects of packing coefficient, Gilbert distance, and Gilbert number on the probability of error. Fairly simple but relatively accurate expressions have been developed to show the increased signal-to-noise ratio required (relative to binary PSK) for the arrays of signal points considered. The asymptotic performances reveal the dramatic power savings inherent in the joint modulation forms.

Acknowledgement The close collaboration of M. K. Simon is greatly appreciated.

References

1. Lucky, R. W. . Salz, J. , and Weldon, E. J. , Jr. , Principles of Data Communication, McGraw-Hill Book Co. , Inc., New York, N. Y. 1968.

[1] I.e., $\log_2 M$.

2. Arthurs, E. , and Dym, H. , “On the Optimum Detection of Digital Signals in the Presence of White Gaussian Noise -- A Geometric Interpretation and a Study of Three Basic Data Transmission Systems,” IRE Trans. Commun. Syst. , December, 1962.

3. Filopowsky, R. F.J. , “Nonbinary Information Transmission,” *Proc. IREE*, Australia, Vol. 30, No. 12, December, 1969.

4. Cahn, C. R. , “Performance of Digital Phase-Modulation Communication Systems,” IRE Trans. Commun. Syst. , pp. 3-6, May, 1959.

5. Cahn, C. R. , “Comparison of Coherent and Phase-Comparison Detection of a Four Phase Digital Signal,” *Proc. IRE* (corresp. Vol. 47, p. 1662, September, 1959.

6. Trabka, E. A. , “Embodiment of the Maximum Likelihood Receiver for Detection of Coherent Pulsed Phase Shift Keyed Signals in the Presence of Additive White Gaussian Noise,” in Investigations of Digital Data Communications Systems, J. G. Lawton, Ed. , Cornell Aeronaut. Lab. , Inc. , Buffalo, N. Y. , Rep. UA-1420-S-1, Detect. Memo 5A, January, 1961.

7. Lindsey, W. C. , and Simon, M. K. , “Carrier Synchronization and Detection of Polyphase Signals,” IEEE Trans. Commun. Tech. , Vol. COM-20, No. 3, June, 1972.

8. Cahn, C. R. , “Combined Digital Phase and Amplitude Modulation Communication Systems,” IRE Trans. Commun. Syst. , September, 1960.

9. Salz, J. , Sheehan, J. R. , and Paris, D. J. “Data Transmission by Combined AM and PM,” Bell Syst. Tech. J., Vol. 50, No. 7, September, 1971.

10. Campopiano, C. N. , and Glazer, B. G. , “A Coherent Digital Amplitude and Phase Modulation Scheme,” IRE Trans. Commun. Syst. , March, 1962.

11. Sakrison, D. J. , Communication Theory: Transmission of Waveforms and Digital Information, John Wiley and Sons, Inc., New York, N.Y. , 1968.

12. Pappenhis, E. W. , Bruene, W. B. , and Schoenike, E. O., Single Sideband Principles and Circuits, McGraw-Hill Book Co. , Inc. New York, N.Y., I964.

13. Hancock, J. C. , and Lucky, R. W., “Performance of Combined Amplitude and Phase-Modulated Communication Systems,” IRE Trans. Commun. Syst., p. 232, December, 1960.

14. Lucky, R. W. , and Hancock, J. C. , “On the Optimum Performance of N-ary Systems having Two Degrees of Freedom,” IRE Trans. Commun. Syst. p. 185, June, 1962.

15. Thomas, C. M. “Amplitude-Phase-Keying with M-ary Alphabets: A Technique for Bandwidth Reductions,” Proc. Int. Telem. Conf. p. 289, 1972.

16. Kawai, K., Shintani, S., and Yanagidaira, H., “Optimum Combination of Amplitude and Phase Modulation Scheme and its Application to Data Transmission Modem,” IEEE Int. Conf. Commun., Conference Record, p. 29-6. 1972.

17. Simon, M. K., and Smith, J. G., “A Hex on MPASK,” submitted for presentation at the IEEE International Conference on Communications, June, 1973.

18. Foschini, G. J., Gitlin. R. D., and Weinstein, S. B. , “On the Selection of a Two-Dimensional Signal Constellation in the Presence of Phase Jitter and Gaussian Noise,” submitted for publication in Bell Syst. Tech. J.

19. Gilbert, E. N., “A Comparison of Signalling Alphabets,” Bell Syst. Tech. J., p. 504, May, 1952.

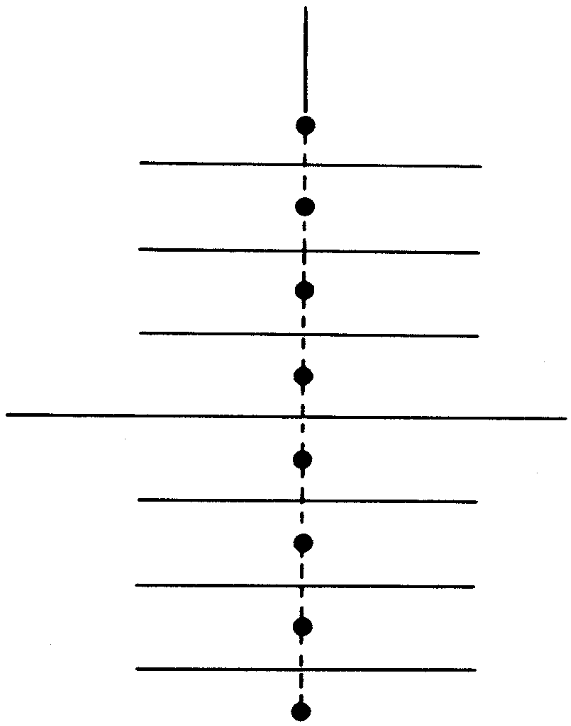

Figure 1. Type 0--octal ASK

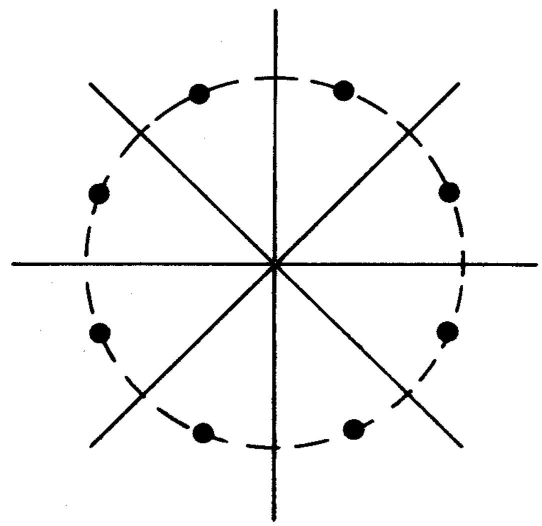

Figure 2. Type 0--octal PSK

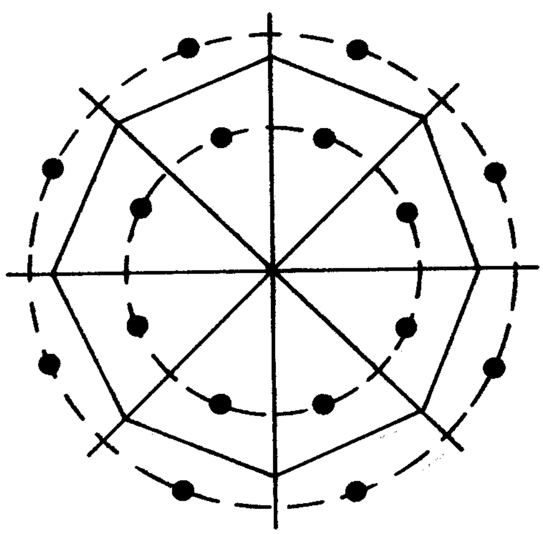

Figure 3. Type I--IAPSK (16)

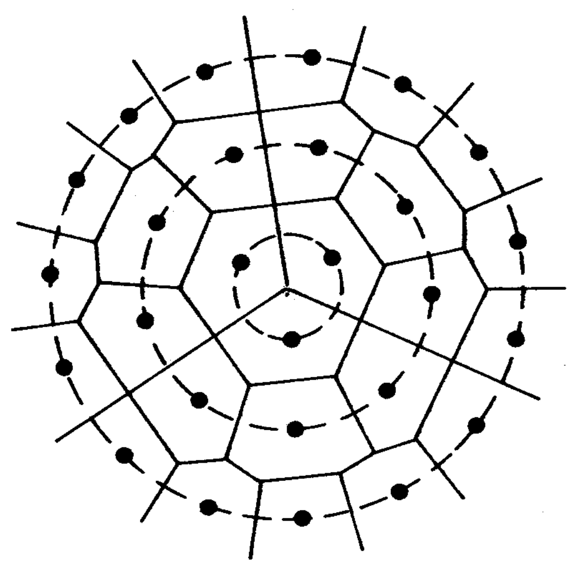

Figure 4. Type H, with three rings

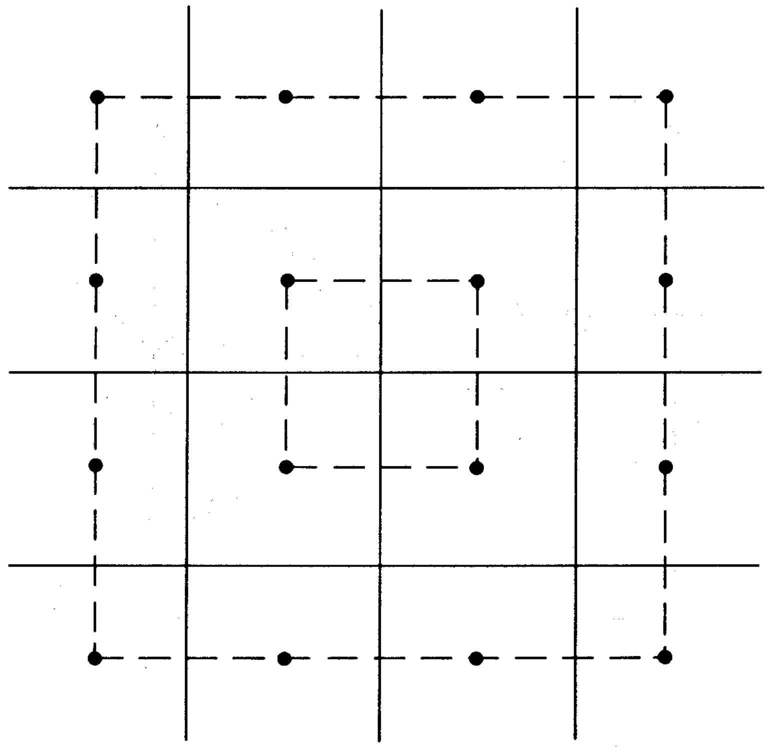

Figure 5. Type III--QASK (16)

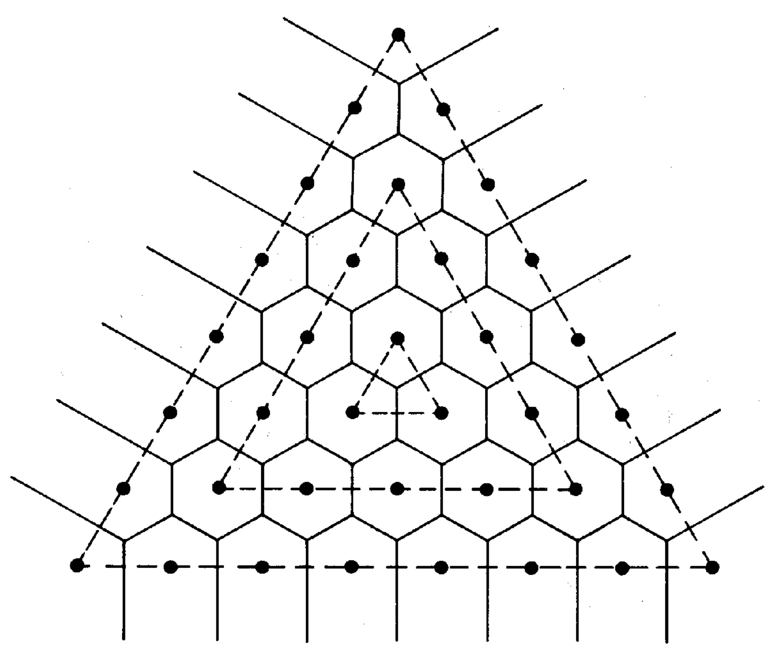

Figure 6. Type IV--concentric triangles

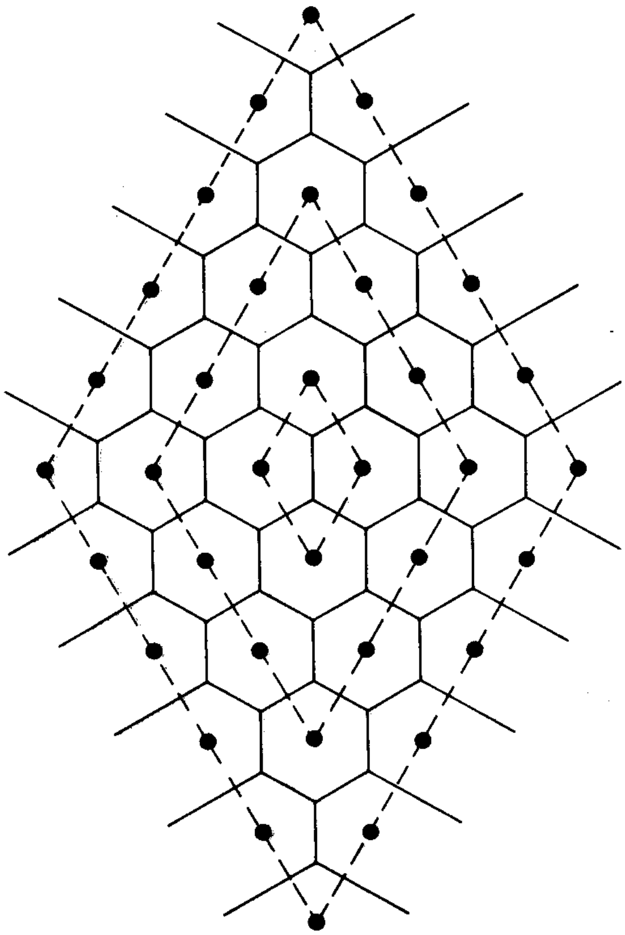

Figure 7. Type IV--concentric diamonds

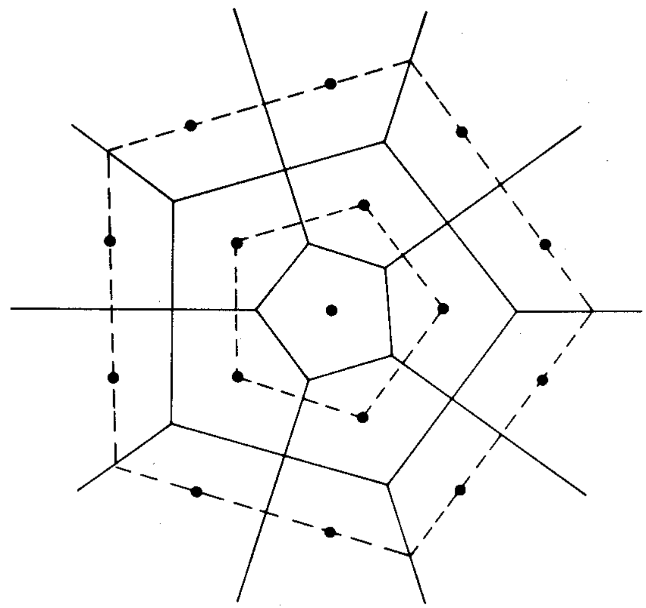

Figure 8. Type IV--concentric pentagons

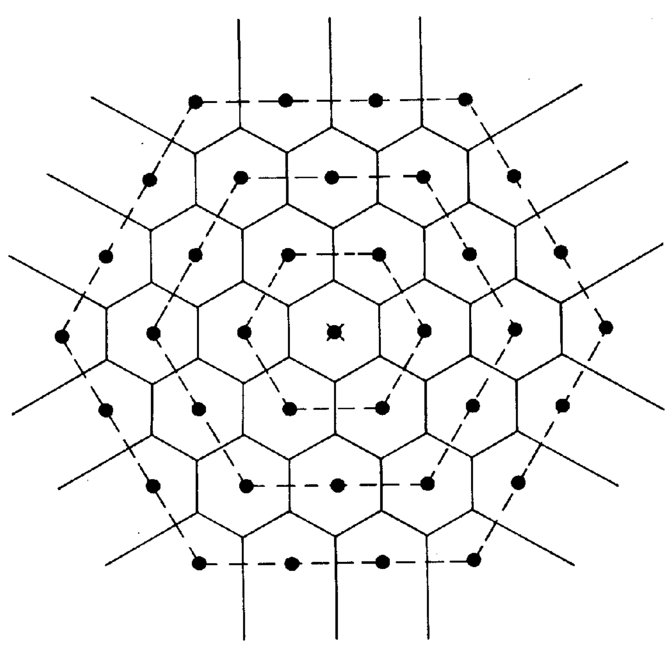

Figure 9. Type IV--concentric hexagons

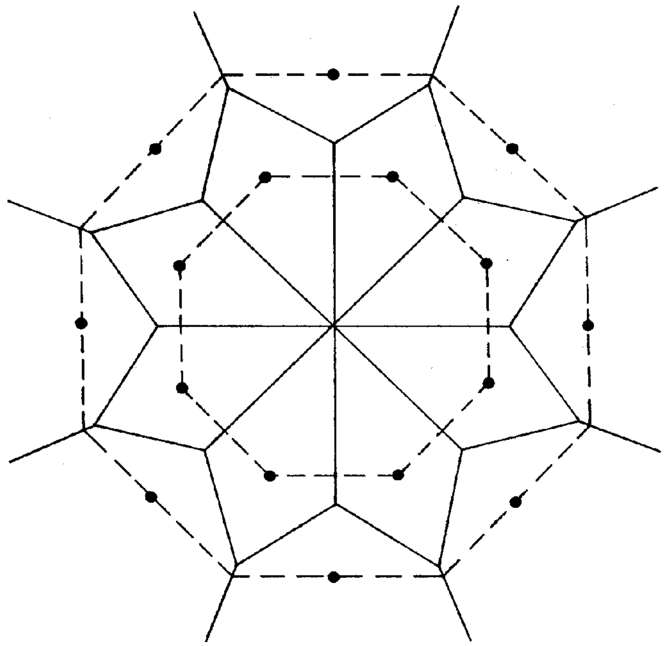

Figure 10. Type IV--concentric octagons

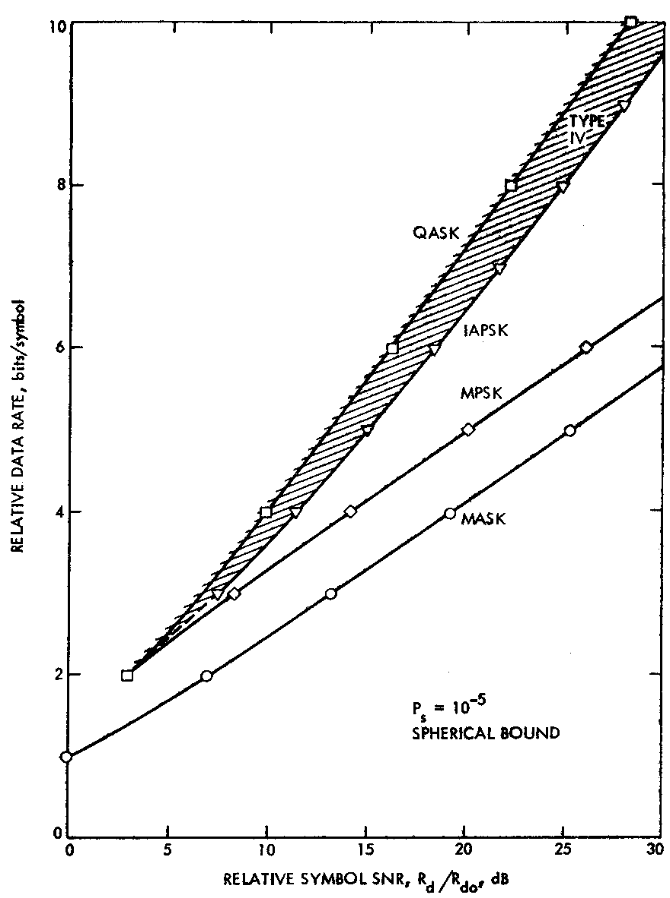

Figure 11. Data rate--symbol energy tradeoff at constant spherical bound ($P_s = 10^{-5}$)

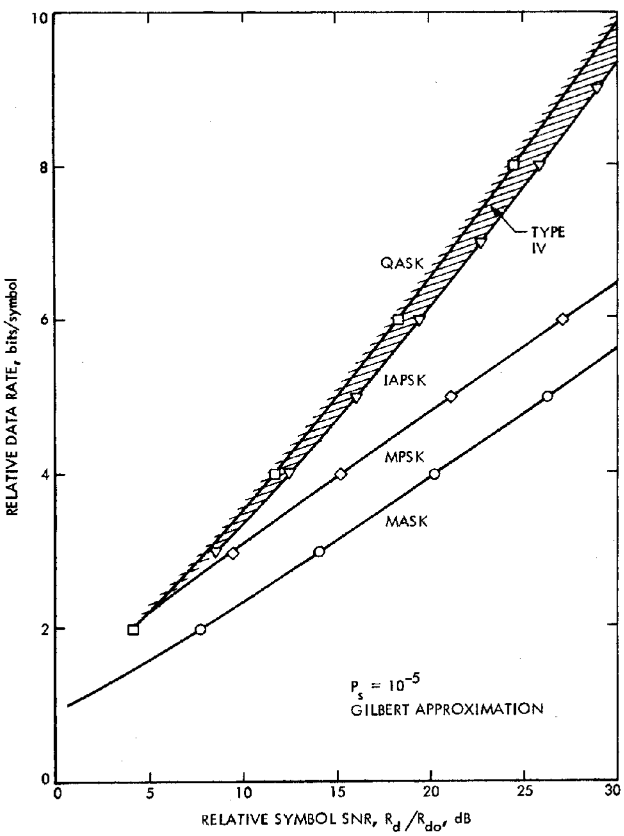

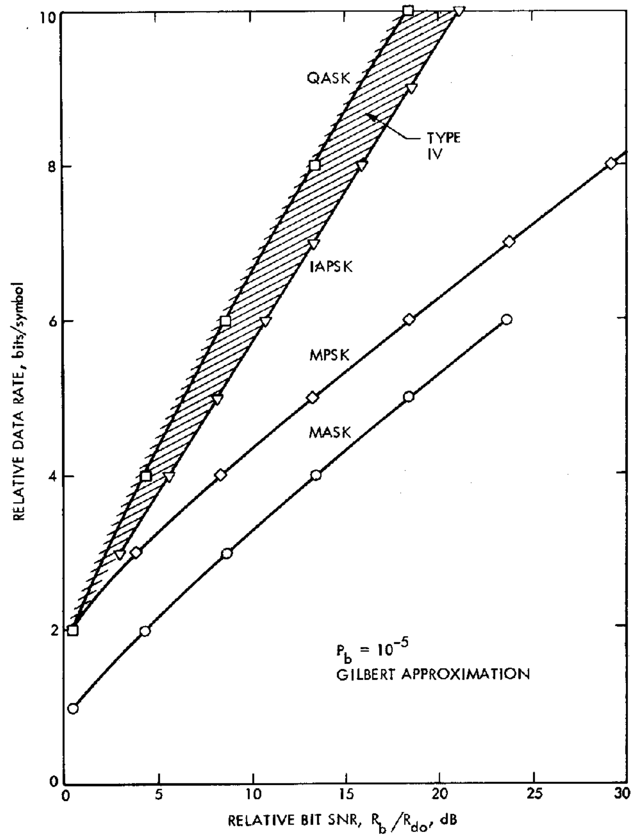

Figure 12. Data rate--symbol energy tradeoff at constant Gilbert approximation ($P_s = 10^{-5}$)

Figure 13. Data rate--bit energy tradeoff at constant Gilbert approximation ($P_b = 10^{-5}$)